Probabilistic Engineering Mechanics 59 (2020) 103037

Contents lists available at ScienceDirect

Probabilistic Engineering Mechanics

journal homepage: www.elsevier.com/locate/probengmech

Lifecycle operational reliability assessment of water distribution networks based on the probability density evolution method

Wei Liu [a,b,*], Zhaoyang Song [b], Zhiqiang Wan [b], Jie Li [a,b]

[a] State Key Laboratory of Disaster Reduction in Civil Engineering, Tongji University, Shanghai 200092, China
[b] Department of Structural Engineering, Tongji University, Shanghai, 200092, China

ARTICLE INFO

Keywords:
Operational reliability
Water distribution networks
Probability density evolution method
Leak
Burst
Lifecycle

ABSTRACT

In this study, a lifecycle operational reliability assessment framework for water distribution networks (WDNs) is proposed on the basis of the probability density evolution method (PDEM). The occurrence models of daily accidents are fitted using the maintenance data provided by a local water administration sector. For a given accident, two types of accidents (e.g., leaks and bursts) are distinguished in different occurrence probabilities and simulated in various ways. The pipe deterioration process in the lifecycle is reflected by incorporating the time-dependent pipe roughness model. Considering various randomness in the model, PDEM, a newly proposed and developed method for a stochastic system, is used to evaluate the lifecycle operational reliability of WDNs. The framework is demonstrated using an actual WDN, and the nodal reliabilities in the lifecycle are obtained. Comparisons of the operational reliabilities of all nodes calculated via the PDEM and Monte Carlo simulations prove that PDEM is an accurate and highly efficient method.

1. Introduction

As an important component of critical infrastructure, water distribution networks (WDNs) are crucial in modern cities not only because they provide water services for domestic and industrial activities but also because they are the foundation of normal operations of other infrastructure systems, such as power and gas systems. Thus, some scholars regard these network systems as urban lifeline systems [1]. Unfortunately, various events, including aging pipes, leaks, bursts, pollution, and water hammer, influence the safe operation of WDNs. According to survey data of a district in Shanghai, China, which has a total pipe length of 248 km, the average number of accidents from 2012 to 2015 was 2256/year as a result of pipe aging, sudden change in temperature, third-party destruction, man-made maloperation, and other factors. These daily accidents cause huge economic losses and decreased quality of life of citizens. Moreover, other infrastructure systems may be affected or even paralyzed. For example, a pipe burst along a main road may cause traffic congestion. A road cave-in caused by long-term water leaks may threaten the surrounding buried pipes/cables. Therefore, evaluating and improving the operational performance of WDNs is essential for local managers, and hence becomes the major motivation of this study.

Reliability of WDNs is a traditional research topic. It can be defined as the probability of satisfying nodal demands and pressure heads under various possible failures at any given time [2]. In terms of failure mechanics, the reliability research of WDNs can be divided into three aspects [3], namely, mechanical (e.g., connectivity from source to node) [4,5], hydraulic (e.g., nodal hydraulic state) [6,7], and water quality (e.g., water quality) [8,9] reliabilities. In recent years, the increasing complexity of engineering systems and their working environments enhance the importance of operational reliability throughout a lifecycle [10], which is also a necessary research topic regarding WDNs.

A major challenge of the lifecycle operational reliability assessment of WDNs is the consideration of multiple simultaneous failures [3]. First, accidents, such as bursts or leaks, may occur simultaneously on different pipes because of the wide distribution of WDNs. Second, different kinds of failures, including leaks, bursts, aging, demand variation, and chlorine decay, are coupled in the lifecycle. In the lifecycle reliability analysis, these conditions should be considered to reflect the real state of WDNs. The complexity of the model poses difficulties in reliability quantification, which is enhanced by randomness. In the lifecycle period, various randomness, such as failure occurrence, type, damage, and location, exist. In previous research, Monte Carlo simulation (MCS) [11], minimum cut set [12], and other mathematical programming methods [13], have been used repeatedly to solve the problem. However, these methods have certain drawbacks. For example, MCS needs to solve a large number of time-consuming nonlinear flow analyses to obtain a precise solution. The minimum cut algorithm increases the difficulty in determining the minimum cut sets of large WDNs and has high computation requirements [14]. In

* Corresponding author at: State Key Laboratory of Disaster Reduction in Civil Engineering, Tongji University, Shanghai 200092, China.
E-mail addresses: liuw@tongji.edu.cn (W. Liu), songzy@tongji.edu.cn (Z. Song), wanzhiqiang@tongji.edu.cn (Z. Wan), lijie@tongji.edu.cn (J. Li).

https://doi.org/10.1016/j.probengmech.2020.103037
Received 15 January 2020; Accepted 29 January 2020
Available online 1 February 2020

addition, some reliability surrogate indices, including entropy [15], energy [16], robustness [17], and resilience [13,18,19] have been proposed with neglecting the analysis of various randomness to a certain degree. Although these indices perform well in some cases, such as the optimization design or surplus evaluation of WDNs, they still differ from the actual system reliability level in terms of probabilistic failure, which is a major source of randomness. The probability density evolution method (PDEM) is a new method for the analysis of stochastic systems that has been proposed and developed in recent years [20]. This method directly obtains the probability density function (PDF) of the target system response by combining the basic random variables with physical equations of the system based on the probability preservation principle. PDEM is fairly accurate and efficient compared with traditional methods [21].

In this study, a lifecycle operational reliability assessment model for WDNs is constructed using the PDEM. The remainder of this work is organized as follows. Section 2 introduces the lifecycle operation simulation models of WDNs, including the accident occurrence models of the three pipe types (i.e., cast iron pipes (CIPs), ductile iron pipes (DIPs), and steel pipes (SPs)), simulation models for two common accidents (i.e., leaks and bursts), and the time-dependent pipe aging model. Section 3 proposes the operational reliability assessment methods, including the concept of operational reliability and the basic theory of the PDEM. In Section 4, the WDN in Mianzhu, China is used as a case to illustrate the aforementioned framework, and the results obtained by the PDEM and MCS are compared. Section 5 draws the conclusion of this study.

2. Lifecycle operation simulation models of WDNs

The operation simulation methods for WDNs during the lifecycle period, including the accident occurrence (Section 2.1), accident simulation (Section 2.2), and pipe aging (Section 2.3) models, are introduced in this section. Note that only pipe accidents are considered in this model under the assumption that no damage will occur in the network nodes.

2.1. Accident occurrence models

Various accidents occur throughout the lifecycle of WDNs. In this study, we only focus on common daily accidents without considering the influence of water quality and natural disasters, such as earthquakes. According to the maintenance data provided by the water administration sector, daily accidents, including leaks and bursts, occur frequently. Generally, the occurrence rates of these accidents are related to several factors, such as pipe age, material, diameter, and environment. However, only two major factors, including pipe material and age, are selected to build the accident occurrence models due to insufficient maintenance data. In this study, three types of pipes, namely, CIPs, DIPs, and SPs, are considered.

2.1.1. CIPs

CIPs are still widely used in many countries because of the historical or economic factors. Previous research has shown that the accident rates of CIPs can be expressed by the following exponential form [22]:

$$N(t) = N(t_0)\, e^{\beta T} \tag{1}$$

where $N(t)$ is the accident rate at year t (/km/year); $N(t_0)$ is the initial accident rate taking t_0 as the base year (/km/year); β is the growth rate coefficient (/year); and T is the pipe age (year) equal to $(t - t_0)$. As suggested by [22], $N(t_0)$ and β can take the values of [0.328, 0.820] and [0.05, 0.15] when the data are insufficient, respectively. Herein, $N(t_0)$ takes the mean value of the recommended range at 0.574/km/year because the records of early pipe accident are limited. We use the maintenance data from 2004 to 2013 to obtain a fitted value for β.

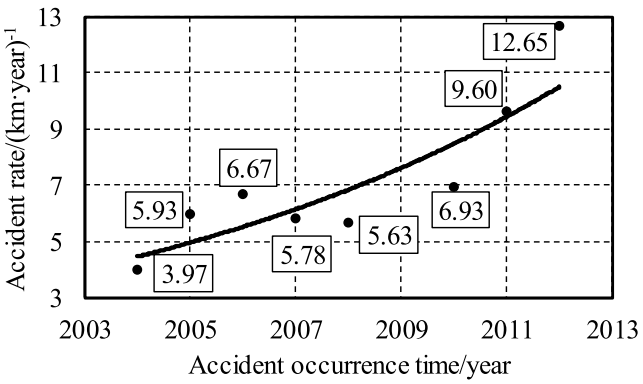

Fig. 1. Fitting of β for CIPs ($R = 0.88$).

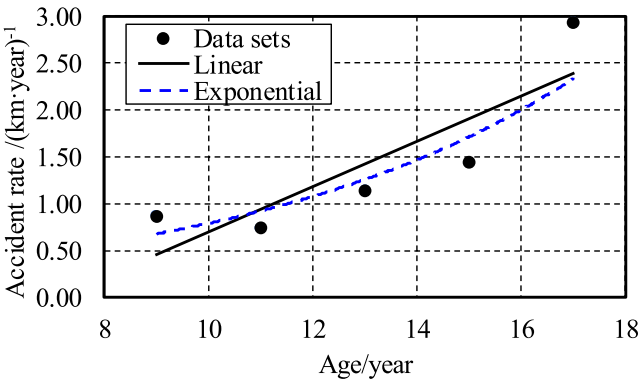

Fig. 2. Fitting of accident rates for DIPs (correlation coefficient of the linear function, $R_L = 0.89$, correlation coefficient of the exponential function, $R_E = 0.91$).

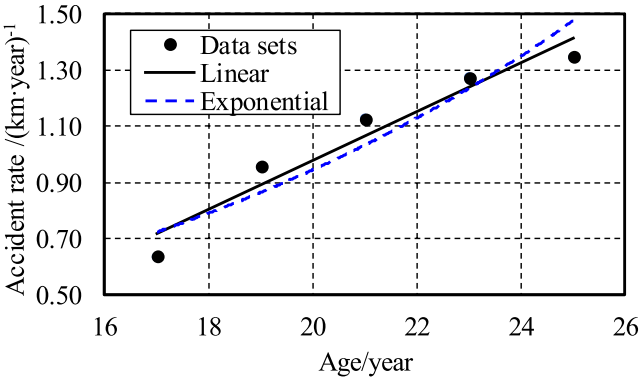

Fig. 3. Fitting of accident rates for SPs ($R_L = 0.97$, $R_E = 0.94$).

Fig. 1 shows that the fitted result is $\beta = 0.11$ with a high correlation coefficient ($R = 0.88$) after two outliers are excluded (2009 and 2013). Note that the accident occurrence time t is used as the transverse axis instead of pipe age T. Thus, Eq. (1) becomes $N(t) = N(t_0)e^{\beta(t-t_0)}$. Although t_0 is unknown in this case, β is still credible because of its independence from t_0. In addition, β should be adjusted on the basis of the local maintenance data because the pipe working environments in different places may vary considerably.

2.1.2. DIPs and SPs

Compared with CIPs, the performance of DIPs and SPs are better and will not deteriorate clearly over time. In this study, the mean accident rates of two adjacent years are used to eliminate data variability. Meanwhile, the pipe ages take the mean values of all the pipes because

their buried time is close to one another. Thus, five data sets are determined to describe the relationship between the pipe accident rates and ages. Herein, two functions, namely, the exponential and linear forms, are selected to build the accident rate models. As shown in Figs. 2 and 3, the two functions fit the data sets with high correlation coefficients. The fitting results of the linear function are presented as follows:

$$\begin{cases} N(t) = 0.242T - 1.720 & \text{DIP} \\ N(t) = 0.087T - 0.758 & \text{SP} \end{cases} \tag{2}$$

The fitting results of the exponential function are presented as follows:

$$\begin{cases} N(t) = 0.167e^{0.155T} & \text{DIP} \\ N(t) = 0.158e^{0.089T} & \text{SP} \end{cases} \tag{3}$$

If we expand the observation period to the entire lifecycle, the effect of linear function is still acceptable. But the exponential function becomes unsatisfactory because it underestimates the pipe performance in the late stage. For example, the accident rate becomes 82/km/year when CIPs operate for 40 years. Then, the accident rates rise to 388 and 14/km/year when CIPs and SPs operate for 50 years, respectively. These results are inconsistent with reality because DIPs and SPs still demonstrate stable performance in the late operation stage, as described by the operators. In addition, when the pipes operate over 28 years, the accident rate of DIPs (13/km/year) even exceeds that of CIPs (12/km/year), which is inconsistent with engineering practice. To overcome the two drawbacks, we select the linear functions in this model. Thus, the performance of DIPs and SPs are stable and will not seriously deteriorate even in the late stage. In addition, the relationships of accident rates of the three types of pipes are also satisfied in the following order: CIPs > DIPs > SPs.

The accident rates of DIPs and SPs are negative in the early stage for the linear functions. This finding corresponds to the first 7 and 8 years for DIPs and SPs, respectively. The problem is solved by substituting the previous negative values with the first positive value calculated via Eq. (2). Then, the annual accident rates are 0.216 and 0.0252/km/year for DIPs and SPs in the first 7 and 8 years, respectively. In this manner, the accident occurrence models are divided into stable and linear growth stages. This two-stage characteristic has been proven in a previous study [23]. However, one difference is that the first stage is accident-free based on their models, whereas a low accident rate is used in our models. In addition, Eq. (2) is fitted with the maintenance data. Thus, some parameters should be adjusted on the basis of local records before they can be used elsewhere.

Eqs. (1) and (2) can be used to obtain the pipe accident rate per kilometer per year. The results are divided by 365 to obtain the accident rate per kilometer per day of a pipe. In this study, pipe accident occurrence is assumed to follow the Poisson distribution. Thus, the accident probability of a given pipe is $P_F = 1 - e^{-\lambda L}$, where λ(/km/day) is the accident rate per kilometer per day, and L is the pipe length. In the same year, P_F of different days are assumed to be equal.

2.2. Accident simulation models

The accident simulation models of different pipes are presented in this section. For a given accident, the specific accident type should be confirmed first. In the maintenance data, leaks and bursts account for 90% and 10% of all records, respectively. Correspondingly, for a pipe with a daily accident probability P_F, the occurrence probabilities for leaks and bursts are assumed to be $0.9P_F$ and $0.1P_F$, respectively. In this study, we simulate leaks and bursts in two different ways.

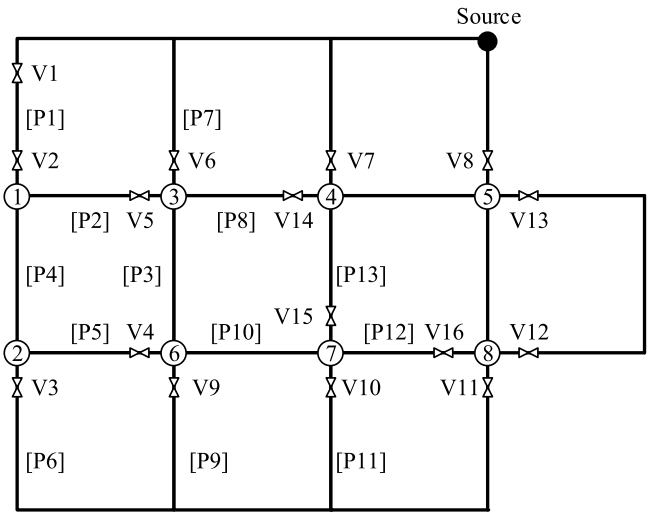

Fig. 4. A small WDN.

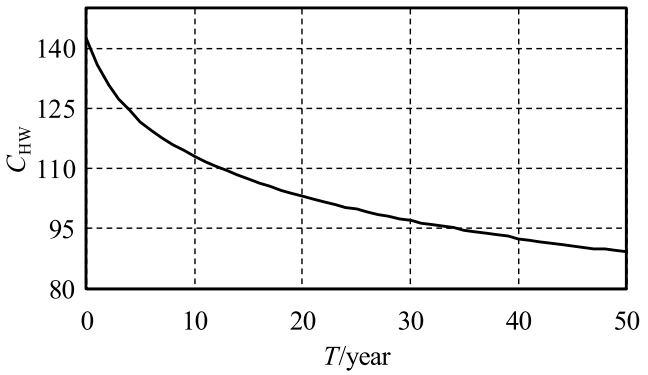

Fig. 5. Deterioration of C_{HW} for a pipe with a diameter of 400 mm.

2.2.1. Leaks

Leaks can occur in pipe joints or walls and are common in the lifecycle operation of WDNs. The pipe transportation capacity decreases when water leaks. Generally, a hydraulic equilibrium equation that considers leak flow can be expressed as [6]:

$$\mathbf{AQ_P} + \mathbf{Q_N} + \mathbf{Q_L} = \mathbf{0} \tag{4}$$

where $\mathbf{A} = [a_{ij}]$ is the connection matrix used for describing the network topology, which takes 1 (water in pipe j flows out of node i), −1 (water in pipe j flows into node i), and 0 (node i is not connected to pipe j); $\mathbf{Q_P}$ is the pipe flow vector; $\mathbf{Q_N}$ is the nodal flow vector; and $\mathbf{Q_L}$ is the leak flow vector. Herein, the following Hazen–Williams equation is selected to describe the relationship between pipe flow and nodal head difference:

$$q_P = 0.278C_{HW}D^{2.63}\Delta H^{0.54}L^{-0.54} \tag{5}$$

where q_P is the pipe flow; C_{HW} is the Hazen–Williams coefficient related to pipe roughness; D is the pipe diameter; ΔH is the pipe head loss measured by head difference of two incident nodes; and L is the pipe length.

The pipe leakage flow is assumed to be borne by the nodes at the two ends of the pipe. Thus, no new equation is needed, and the error is accepted [6]. Herein, the following modified point leakage model is adopted [1].

$$q_L = 0.6\varphi A_L\sqrt{2gH_L} \tag{6}$$

where q_L is the leakage flow; φ is the leak coefficient, which can take 0.1–0.3 when data are insufficient; g is the gravity acceleration;

H_L is the head of the leak point; and A_L is the leak area. In this study, the randomness of A_L is considered and assumed to satisfy the uniform distribution in [0.1%, 20%]· S, where S is the pipe section area. This consideration is practical because a small leak (<0.1%S) is difficult to detect and has minimal influence on the pipe hydraulic state. Meanwhile, when A_L is larger than 20%S, operators usually treat it as bursts.

2.2.2. Bursts

Burst is another common accident in the operation of WDNs. After its occurrence, the first task is to isolate the accident pipe by closing the valves. If the relevant valves are not determined timely, then a considerable amount of water will be lost and lead to substantial water waste and even secondary effects, such as head drop of neighboring consumers and local traffic congestion. Many efficient valve closure strategies have been introduced and successfully applied in practice with the development of computer technology [24,25]. In this study, an algorithm based on the depth-first search is used and demonstrated with a small WDN (Fig. 4). Generally, three valve configurations should be considered for bursts.

(1) Two valves locate on both sides of the burst point. For example, if a burst occurs in pipe P1, then valves V1 and V2 should be closed to isolate the accident. Note that the burst is assumed to occur between the two valves in this case; otherwise, the burst is treated as Case (2).

(2) One valve exists in the accident pipe. For example, if a burst occurs in pipe P2, then valves V2–V5 should be closed. The specific search steps based on the depth-first algorithm are presented as follows: First, close valve V5 and mark pipe P2 as visited. Second, begin the search by taking node 1 as the starting point, and search one pipe connected to it (P1). Given that valve V2 locates on pipe P1, close V2 and mark P1 as visited. Third, return to node 1 and search for the other unvisited pipes connected to it (P4). No valve exists on P4. Thus, it must be marked as visited, and node 2 should be selected as the starting point to deepen the search. The same process is repeated until all relevant valves are determined and node 1 is isolated. Finally, the pipe search sequence is P2, P1, P4, P6, P5, and the valve closure sequence is V5, V2, V3, V4. The basic principles of the above search are similar to that of the depth-first search algorithm. However, four points should be emphasized. First, mark the pipe as visited after its search is completed regardless of whether a valve exists or not. Second, the visited pipes cannot be searched repeatedly. Third, the search will deepen continuously unless the stop criteria are satisfied, that is, a valve is searched or the pipe is located at the end of the path. Fourth, once the stop criteria are satisfied, return to the upstream nodes with unvisited pipes and continue the search.

(3) No valve exists on the accident pipe. For example, if a burst occurs in pipe P3, then valves V4, V5, V6, V9, V10, V14, V15, and V16 should be closed. The specific search steps are presented as follows: Mark pipe P3 as visited and perform the search independently by taking nodes 3 and 6 as the starting points. For any search, the steps are similar to those of Case (2). Thus, the pipe search sequence starting at node 3 is P2, P7, P8. The corresponding valve closure sequence is V5, V6, V14. The pipe search sequence starting at node 6 is P5, P9, P10, P11, P12, P13. The corresponding valve closure sequence is V4, V9, V10, V16, V15. Finally, all valves to be closed are the union of the above two research results.

Some valves determined by the above method may be redundant. For example, if valves V14–V16 do not exist, then the identified valves to be closed after a burst occurs in P3 are V4–V13. From the perspective of reliability between the isolated nodes (nodes 3–8) and source, valves V4–V11 must be closed, whereas valves V12 and V13 are redundant. The redundant valves should be excluded to improve the working efficiency in practice although their closure has no influence on the reliability evaluation. A feasible solution that determines the redundant valves is to open the valves alternately (V4–V13). Then, judge the connectivity between the isolated nodes (nodes 3–8) and the source. If the nodes are still unconnected, then the valve is redundant and vice versa.

2.3. Pipe aging model

Pipe aging comes from two aspects. First, the pipe eternal wall corrodes due to long-term environmental influence. Then, certain zones, including the joints or welds, may become vulnerable to accidents. Leaks or bursts are likely to occur once the operational condition, such as third-party disturbance or man-made maloperation, changes. These changes are introduced in Section 2.2. Second, the roughness of the pipe inner wall increases under long-term water erosion and reduces C_{HW} in Eq. (5) and pipe transportation capacity. C_{HW} is generally difficult to measure but can be recalculated by using some measurable parameters, such as the absolute roughness coefficient e. In this study, the relationship between C_{HW} and e proposed by Sharp and Walski is used as follows [26]:

$$C_{HW} = 18.0 - 37.2 \log \frac{e}{D} \tag{7}$$

$$e = e_0 + aT \tag{8}$$

where e_0 is the initial e for a newly buried pipe. Generally, e_0 should be determined with a test. In case of insufficient data, the different pipes can take the values suggested in [27]. a is the annual growth rate of e. Cement or plastic pipes takes the value of 0 because the pipe internal roughness changes slowly during the lifecycle [26]. Metal pipes can be expressed as $a = 10^{-(4.08+0.38LI)}$, where LI is the Langelier index relevant to the water quality, which is a negative or positive value for corrosive or scale-forming water, respectively. LI in tap water transported in the WDNs can take the value of −1.5.

Fig. 5 shows the exponential deterioration process of C_{HW} for a metal pipe with a diameter of 400 mm. Compared with the initially buried year (C_{HW} = 143), it drops by 38% after the pipe has operated for 50 years (C_{HW} = 89). The pipe flow is still reduced by the same percentage, thereby further influencing the nodal head connected to the pipe based on Eq. (5).

3. Operational reliability assessment framework of WDNs

3.1. Concept of operational reliability

The reliability of an engineering structure is defined as the probability of completing the scheduled function at a given period and condition [28]. According to this definition, the lifecycle operational reliability of WDNs can be measured by using the probability of satisfying the consumers' water requirements at various operational conditions during the entire lifecycle period. In this study, instead of the overall reliability of WDNs, we focus on the reliability of each consumer node. Thus, the operational states of all nodes are clearly shown. In practice, the water demand of a given consumer node is influenced by the obtained head. When the obtained head exceeds the demand head, consumers can always obtain sufficient water and vice versa [6]. Thus, the nodal operational reliability can be written as

$$R_{i,t} = \Pr\left(H_{i,t} \geq H_{i,t}^0\right) \tag{9}$$

where $R_{i,t}$ is the reliability of node i at time t; $H_{i,t}$ is the nodal head; and $H_{i,t}^0$ is the minimum demand head. This general equation incorporates the supply (WDNs) and demand (consumers) sides. For the supply side, the influences of various accidents and pipe aging are embodied in $H_{i,t}$. For the demand side, the demand change in consumers are reflected in $H_{i,t}^0$.

3.2. Probability density evolution method

In engineering, most nonlinear stochastic dynamic systems are conservative. For these systems, the probability conservation principle is valid when no additional random factors appear or disappear in the system evolution process [29]. Li and Chen [20,21] recently proposed

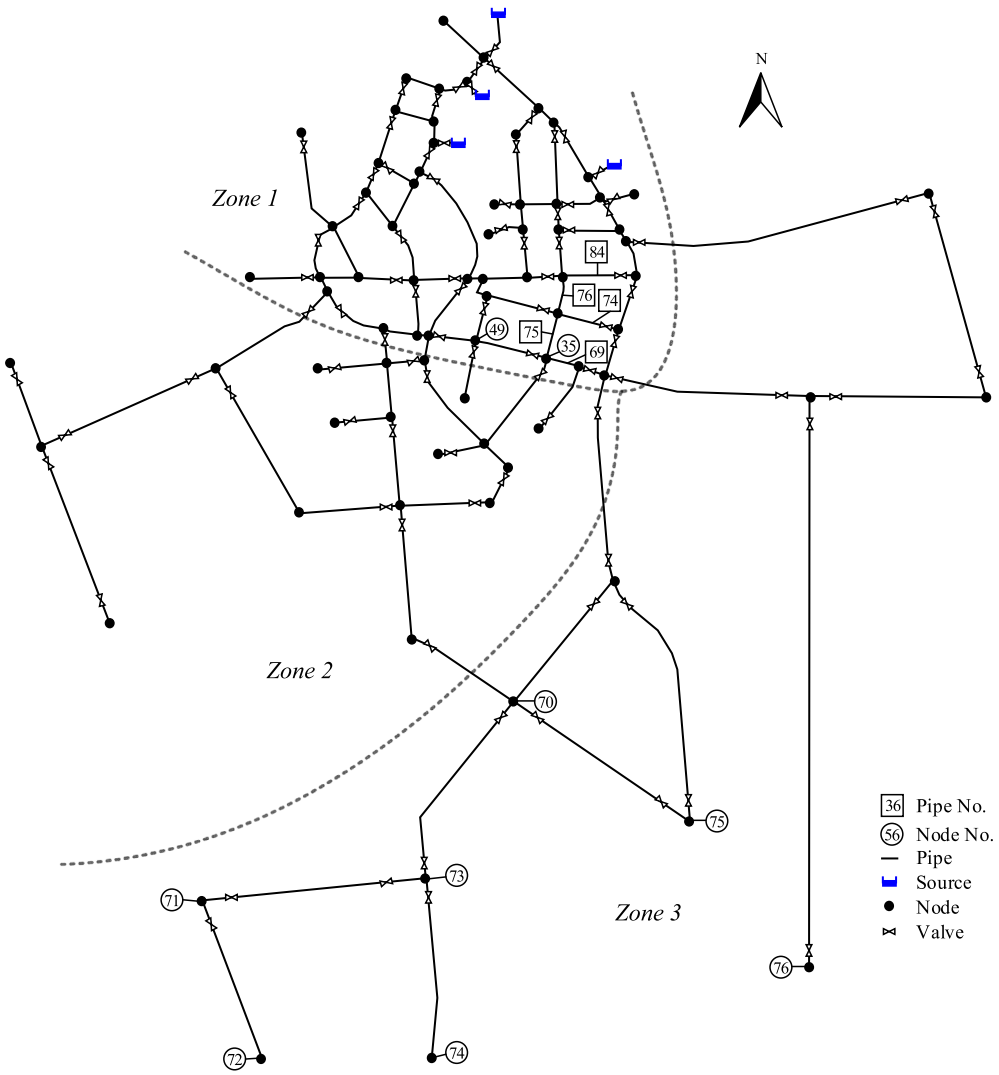

Fig. 6. The WDN in Mianzhu City. Parameters, such as local topology and valve configuration, are changed due to secrecy issues.

and developed PDEM starting with the principle of probability conservation. Compared with MCS, PDEM directly gives the PDF of system response with high accuracy and efficiency. In this study, the system response $X(t)$ is generally expressed as a function of several basic random variables as follows:

$$X(t) = H(\boldsymbol{\Theta}, t) \tag{10}$$

where $\boldsymbol{\Theta} = (\Theta_1, \Theta_1, \ldots, \Theta_s)$ is a basic random vector that comprises all basic random variables of a system; s is the number of the basic random variables; and t is the time. Correspondingly, the velocity process can be obtained as follows:

$$\dot{X}(t) = h(\boldsymbol{\Theta}, t) \tag{11}$$

where $h(\boldsymbol{\Theta}, t)$ is the derivate of $H(\boldsymbol{\Theta}, t)$ with respect to time t. Therefore, for the system expressed by Eq. (10), the corresponding augmented system $(X, \boldsymbol{\Theta})$ is also conservative because all randomness is incorporated in it. Thus, a probability density evolution equation (PDEE) can be expressed as

$$\frac{\partial p_{X\boldsymbol{\Theta}}(x, \boldsymbol{\theta}, t)}{\partial t} + h(\boldsymbol{\theta}, t) \frac{\partial p_{X\boldsymbol{\Theta}}(x, \boldsymbol{\theta}, t)}{\partial x} = 0 \tag{12}$$

The initial condition is

$$p_{X\boldsymbol{\Theta}}(x, \boldsymbol{\theta}, t)\big|_{t=t_0} = \delta(x - x_0)\, p_{\boldsymbol{\Theta}}(\boldsymbol{\theta}) \tag{13}$$

where δ is the Dirac function; and x_0 is the initial value. By solving Eq. (12), PDF of X can be expressed as

$$p_X(x, t) = \int p_{X\boldsymbol{\Theta}}(x, \boldsymbol{\theta}, t)\, d\boldsymbol{\theta} \tag{14}$$

Then, the cumulative density function can be expressed as

$$F_X(x, t) = \int_{-\infty}^{x} p_X(x, t)\, dx \tag{15}$$

Herein, we focus on the nodal head because it directly determines the operational reliability of the node. Note that the water head for a node is a random variable and not a stochastic process. Thus, PDEM cannot be used directly because the "velocity" item in Eq. (11) cannot be quantified. According to Chen and Li [30], a virtual stochastic process could be constructed in such a way that the value under investigation was equal to the value of the virtual stochastic process at a certain "instant of time". Thus, the form of the chosen virtual stochastic process can be arbitrary in principle [31]. In this study, PDEE in Eq. (12) is used by multiplying the nodal head Y by a sine time process to build a virtual stochastic process $X(t)$ as follows [32].

$$X(t) = H(\boldsymbol{\Theta}, t) = Y \sin(0.1\pi t) \tag{16}$$

PDF of X can be obtained by solving Eq. (14). Then, PDF of the nodal head can be calculated by letting $t = 5$ s.

$$p_Y(y) = p_X(x, t)\big|_{t=5} \tag{17}$$

Then, PDF of Y can be obtained. According to Eq. (9), the node is reliable only if the obtained head is larger than the demand head. Thus, nodal reliability is obtained with

$$R_i = \int_{H_i^0}^{+\infty} p_Y(y)\,dy \tag{18}$$

4. Case study: WDN in Mianzhu city

The lifecycle operational reliability assessment framework introduced in Sections 2 and 3 is illustrated in this section by using an actual WDN in Mianzhu, China. Fig. 6 shows that four sources located north of the WDN provide water services to the city with a service area of 1245 km^2 and capacity of 35,000 tons/day. The total length of the main pipes (diameter D ≥ 150 mm) is 44 km. After simplification, 82 nodes, 107 pipes, and 92 valves are included in the model. Given that CIPs are buried in three groups based on the original pipe layout scheme, WDN can be generally divided into three zones. Zone 1 refers to the central area of the city, and CIPs are buried 17 years ago. Zones 2 and 3 are the suburban areas, and the CIPs have served for 16 and 15 years, respectively. Five pipe types of WDN are shown in Table 1. We assume that the initial ages of DIPs and SPs are 0 because of their recent embedding.

Herein, some assumptions and parameters are summarized as follows:

(1) For comparative analysis, the demand head $H_{i,t}^0$ in Eq. (9) takes 20 m without considering the difference in nodes and variation with time.

(2) The operation time of WDN is 40 years to date. Thus, all CIPs can reach the 50-year design working life because of the initial ages [33]. Reliability of WDN is evaluated every 5 years to show the performance deterioration process.

(3) The accident rate per day is adopted and can be obtained by dividing the annual accident rate by 365. For example, for a CIP with 1000 m, the accident rate on the 20th year can be obtained by Eq. (1) ($0.574 \times e^{0.11\times20} = 5.2$/year/km). Then, the accident rate per day is $\lambda = 5.2/365 = 0.0142$/day/km. Based on the Poisson distribution, the daily pipe accident probability is $P_F = 1 - e^{-0.0142\times1.0} = 0.0141$. In addition, pipe roughness is assumed to remain unchanged in the same year. Thus, the annual operational reliability can be represented by the corresponding operational reliability in each day. In other words, the pipe accident rates in different days within the same year are the same, and the corresponding pipe accidents are independent. Note that the correlation in pipe accidents within the same year may exist because the repair of a pipe can influence its performance and the subsequent accident rate. Given the absence of an appropriate model in existing studies and the limited data, they are ignored in this study.

(4) The operation state of a pipe is determined by the two basic random variables of A_S and A_L. A_S is used to evaluate the accident situation (no accident, leak, and burst). Specifically, for the pipe with accident probability P_F, the corresponding probabilities for no accident, leak, and burst are $1 - P_F$, $0.9P_F$, and $0.1P_F$, respectively. On this basis, three intervals (e.g., 0 to $1 - P_F$, $1 - P_F$ to $1–0.1P_F$, and $1–0.1P_F$ to 1) can be obtained. Then, the pipe operational states can be determined by using the interval in which the randomly generated A_S lies. In addition, A_L is used to determine the leak area. Although A_L only functions when a leak occurs, we generate it for all situations to ensure probability conservation during the system evolution. Thus, by considering the 5 pipe types, 10 basic random variables, with 2 for each pipe type, are considered in this case. In this study, A_S and A_L are two random variables uniformly distributed in [0, 1] and [0.1%, 20%]S, respectively.

The basic steps for the lifecycle operational reliability assessment of the Mianzhu WDN in a given year are presented as follows: (1) Select 500 representative points using the GF-discrepancy method [34]. Each point with an assigned probability comprises 10 random values, which are generated on the basis of the distribution types of the 10 basic random variables. (2) Calculate the accident probabilities of all the pipes of WDN and generate the three corresponding intervals. Determine the pipe operational state according to the interval the random values lie in. Thus, a deterministic system is constructed. In this study, 500 deterministic systems are derived. (3) Solve Eq. (4) to obtain the nodal heads for one deterministic system. (4) Construct a virtual stochastic process expressed by Eq. (16) and solve the PDEE. (5) Assemble the results to obtain the PDF of $X(t) = Y\sin(0.1\pi t)$. Then, use Eqs. (17) and (18) to obtain the PDF of Y and the nodal operational reliability, respectively.

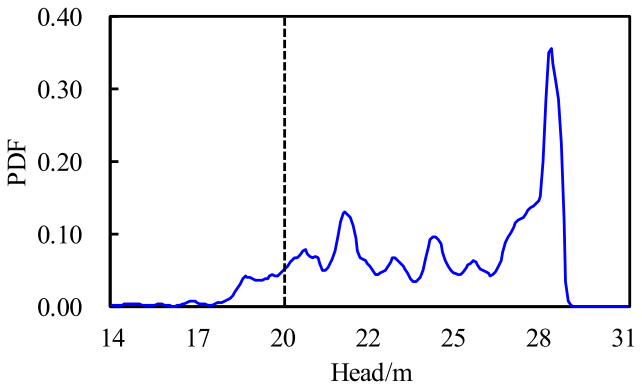

Fig. 7. PDF of node 76 in the 35th year.

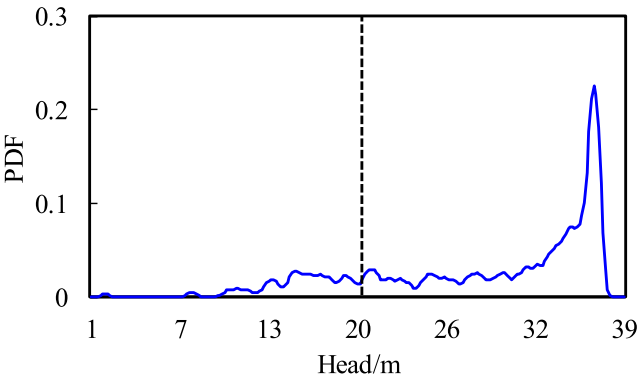

Fig. 8. PDF of node 72 in the 40th year.

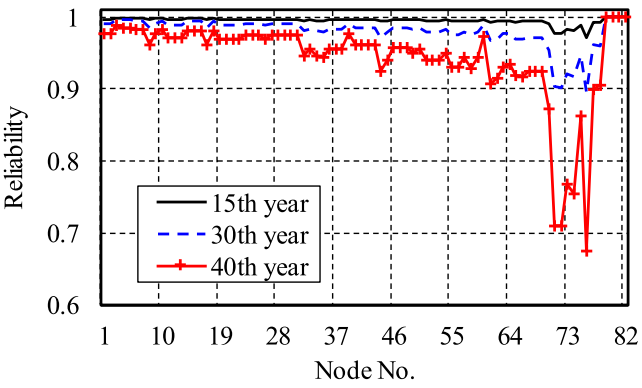

Fig. 9. Nodal reliability in the 15th, 30th, and 40th years.

Instead of focusing on the network as a whole, we pay attention to the reliability of every node to determine the vulnerable nodes. The PDFs of the obtained head for all nodes can be given by using PDEM. As two examples, nodes 76 (35th year) and 72 (40th year) are shown in Figs. 7 and 8, respectively. Instead of a unimodal normal

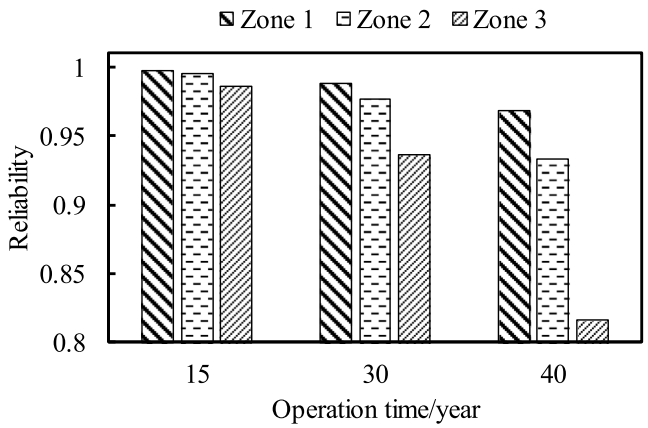

Fig. 10. Mean reliability levels of the nodes in Zone 1–3.

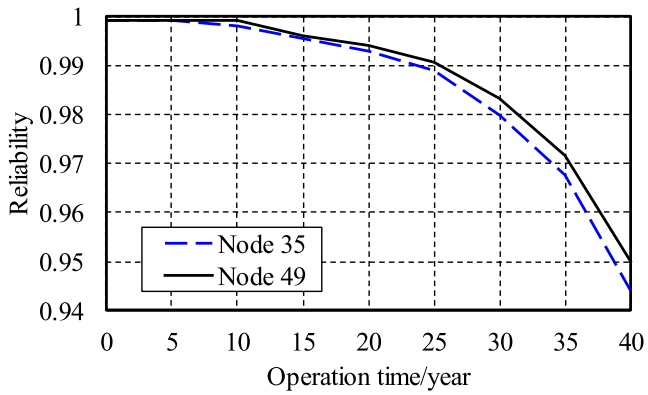

Fig. 11. Comparisons of the reliabilities of nodes 35 and 49.

distribution, the PDFs show evident multimodal characteristics. On the basis of Eq. (18), the reliabilities of the two nodes can be obtained by integrating the PDFs in [20, +∞), which are 0.820 and 0.709, respectively. Accordingly, the reliabilities of the other nodes in different years are calculated with the same method. As shown in Fig. 9, the operational performance of WDN deteriorates with time because of the increasing pipe accident rates and pipe roughness. In the 15th year, the high level of nodal reliability is maintained because only two accidents occur per day according to Eqs. (1) and (2). In the 30th year, although 10 accidents occur per day, reliabilities of all the nodes are acceptable (the minimum is 0.896) because of the well-looped topology and water supply of four sources. In the 40th year, the performance of WDN clearly decreases, and the reliability levels of part nodes, such as nodes 70–76, are even less than 0.8. In this period, the average accident number reaches 30/day. Meanwhile, the increase in pipe roughness further deteriorates the performance of WDN.

The reliability levels of the nodes distributed in Zones 1–3 vary considerably. In this study, the mean reliability levels of the nodes are analyzed, and their individual differences are neglected (Fig. 10). In Zone 1, the mean nodal reliability in the lifecycle period is high because they are close to the sources, and the pipes are well looped. In Zone 2, although the mean nodal reliability decreases, the value is still acceptable and reaches 0.934 in the 40th year. Compared with Zone 1, the nodes in Zone 2 are farther from the sources, but most of them can obtain enough water from the water supply of four sources. In Zone 3, the mean nodal reliability clearly decreases because (1) these nodes are in the tree-like areas of WDN and are thus influenced remarkably by the failures in the upstream pipes; and (2) the pipe connected to them is long and leads to serious on-way head loss. The influences will be magnified clearly once an accident occurs.

Table 1
Pipe types and parameters.

Pipe type	Pipe material	Initial age/years	Length/km
1	CIPs	15	15.3
2	CIPs	16	9.4
3	CIPs	17	15.5
4	DIPs	0	1.1
5	SPs	0	2.8

In addition to the pipe loop configuration and the distance from the source, the valve condition also influences nodal reliability after the occurrence of bursts. For example, nodes 35 and 49 have similar distances from the source and loop configurations, but the reliability of node 35 is still lower than that of node 49 (Fig. 11). Node 49 does not receive water only if bursts occur in the four adjacent pipes because at least one valve is configured in these pipes. However, node 35 is also influenced by some distant pipes, such as pipes 74, 76, and 84, because pipes 69 and 75 have no valves. The influence of valve distribution has become evident in the last 10 years because of the increasing burst occurrence rate.

Overall, the performance of this WDN is still acceptable during the lifecycle period with 50 years as the design working life. The reliabilities of most nodes are more than 0.9 because of the water supply from four sources and looped pipes in most areas. For vulnerable areas, such as nodes 70–76, some enhanced strategies should be applied when the WDN operates for more than 30 years.

In this study, MCS is used to validate the results obtained via the PDEM. In each simulation, the models of pipe accident occurrence, accident simulation, and pipe aging are the same as those of PDEM. However, the final nodal reliability is equal to the ratio of the qualified simulation times ($H \geq 20$ m) to the total simulation times. For MCS, 5000 simulations are repeated to obtain a precise result. The operational reliabilities of some nodes obtained via the PDEM and MCS are listed in Table 2. The accuracy of PDEM is clearly high because all relative errors taking the results obtained by MCS as the benchmark are low. The mean relative error of all nodes during the lifecycle is only 0.12%, and the maximal relative error appearing in node 76 in the 40th year is 3.99%. In addition, PDEM is more effective because only 500 time-consuming analyses of nonlinear flow are needed, whereas 5000 nonlinear flow analyses are required in MCS. The total computation time, including all nodes in the lifecycle, is 13.5 h for MCS but only 1.2 h for PDEM.

5. Conclusions

A PDEM-based lifecycle operational reliability assessment framework for WDNs is established in this study. The proposed framework includes accident occurrence, accident simulation, and pipe aging models. The operational reliability of WDNs in the lifecycle period is then evaluated via the PDEM. By taking the WDN in Mianzhu as an example, we illustrate the above framework and compare the results of PDEM and MCS. The results show that (1) the operational reliability of nodes decreases as time increases, especially in the last 10 years; (2) the distance between the node and the sources, the loop configuration of surrounding pipes, and the valve configuration influence the nodal operational reliability; and (3) PDEM is more accurate than the MCS method. The mean and maximal relative errors in the operational reliabilities of all nodes in the lifecycle are 0.12% and 3.99%, respectively. In addition, PDEM is highly efficient because it avoids the analysis of substantial nonlinear flow. For this case, the total computation time for MCS is 13.5 h but only 1.2 h for PDEM.

Table 2
Comparisons of the operation reliabilities of partial nodes calculated by the PDEM and MCS.

Node No.	15th year			30th year			40th year		
	PDEM	MCS	Relative error/%	PDEM	MCS	Relative error/%	PDEM	MCS	Relative error/%
1	0.9975	0.9986	−0.11	0.9911	0.9916	−0.05	0.9781	0.9758	0.24
4	0.9993	0.9988	0.05	0.9961	0.9954	0.07	0.9857	0.9842	0.16
7	0.9993	0.9988	0.05	0.9939	0.9944	−0.05	0.9829	0.9822	0.07
10	0.9993	0.9988	0.05	0.9939	0.9944	−0.05	0.9829	0.9822	0.07
13	0.9975	0.9978	−0.03	0.9896	0.9902	−0.06	0.9719	0.9708	0.12
16	0.9993	0.9988	0.05	0.9939	0.9934	0.05	0.9809	0.9786	0.23
19	0.9975	0.9976	−0.01	0.9884	0.9884	0.00	0.9695	0.9684	0.12
22	0.9975	0.9976	−0.01	0.9884	0.9884	0.00	0.9695	0.9684	0.12
25	0.9975	0.9980	−0.05	0.9911	0.9906	0.05	0.9759	0.9734	0.25
28	0.9975	0.9980	−0.05	0.9911	0.9906	0.05	0.9759	0.9734	0.25
31	0.9975	0.9980	−0.05	0.9911	0.9902	0.09	0.9746	0.9722	0.25
34	0.9955	0.9958	−0.03	0.9811	0.9810	0.01	0.9469	0.9444	0.26
37	0.9961	0.9966	−0.05	0.9829	0.9826	0.03	0.9566	0.9550	0.17
40	0.9975	0.9974	0.01	0.9857	0.9860	−0.03	0.9625	0.9612	0.13
43	0.9975	0.9974	0.01	0.9857	0.9860	−0.03	0.9625	0.9612	0.13
46	0.9975	0.9970	0.05	0.9852	0.9876	−0.25	0.9585	0.9588	−0.03
49	0.9962	0.9968	−0.07	0.9833	0.9854	−0.21	0.9501	0.9522	−0.22
52	0.9955	0.9956	−0.01	0.9798	0.9808	−0.10	0.9400	0.9418	−0.19
55	0.9943	0.9944	−0.01	0.9764	0.9766	−0.02	0.9300	0.9292	0.08
58	0.9943	0.9944	−0.01	0.9764	0.9762	0.02	0.9286	0.9272	0.16
61	0.9926	0.9944	−0.18	0.9673	0.9632	0.43	0.9075	0.9114	−0.43
64	0.9955	0.9948	0.07	0.9774	0.9780	−0.06	0.9350	0.9340	0.11
67	0.9943	0.9942	0.01	0.9714	0.9728	−0.14	0.9242	0.9220	0.24
70	0.9913	0.9916	−0.03	0.9532	0.9484	0.50	0.8729	0.8780	−0.58
73	0.9836	0.9858	−0.23	0.9210	0.9084	1.39	0.7672	0.7620	0.68
76	0.9712	0.9802	−0.92	0.8965	0.8818	1.66	0.6751	0.7032	−3.99
Time (min)	6	82	–	8	98	–	11	113	–

Acknowledgments

The supports from the National Key Research and Development Program of China (Grant No. 2016YFC0802400), the National Natural Science Foundation of China (Grant No. 51720105005), and the Ministry of Science and Technology of China (SLDRCE19-B-24) are greatly appreciated.

References

[1] J. Li, Lifeline Earthquake Engineering-Basic Methods and Applications, Science Press, Beijing, 2005, (in Chinese).
[2] D.S. Shinstine, I. Ahmed, K.E. Lansey, Reliability/availability analysis of municipal water distribution networks: Case studies, J. Water Res. Plan. Manage. 128 (2) (2002) 140–151.
[3] A. Gheisi, M. Forsyth, G. Naser, Water distribution systems reliability: a review of research literature, J. Water Res. Plan. Manage. 142 (11) (2016) 04016047.
[4] A. Yazdani, P. Jeffrey, Water distribution system vulnerability analysis using weighted and directed network models, Water Resour. Res. 48 (6) (2012) W06517.
[5] A. Agathokleous, C. Christodoulou, S.E. Christodoulou, Topological robustness and vulnerability assessment of water distribution networks, Water Resour. Manage. 31 (12) (2017) 4007–4021.
[6] W. Liu, Y.G. Zhao, J. Li, Seismic functional reliability analysis of water distribution networks, Struct. Infrastruct. Eng. 11 (3) (2014) 363–375.
[7] Q. Shuang, M.Y. Zhang, Y.B. Yuan, Node vulnerability of water distribution networks under cascading failures, Reliab. Eng. Syst. Saf. 124 (2014) 132–141.
[8] R. Farmani, G. Walters, D. Savic, Evolutionary multi-objective optimization of the design and operation of water distribution network: total cost vs. reliability vs. water quality, J. Hydroinform. 8 (3) (2006) 165–179.
[9] R. Portielje, T. Hvitved-Jacobsen, K. Schaarup-Jensen, Risk analysis using stochastic reliability methods applied to two cases of deterministic water quality models, Water Res. 34 (1) (2000) 153–170.
[10] E. Zio, Reliability engineering: old problems and new challenges, Reliab. Eng. Syst. Saf. 94 (2) (2009) 125–141.
[11] A. Ostfeld, Reliability analysis of water distribution systems, J. Hydroinform. 6 (4) (2004) 281–294.
[12] S. Yannopoulos, M. Spiliotis, Water distribution system reliability based on minimum cut – set approach and the hydraulic availability, Water Resour. Manage. 27 (6) (2012) 1821–1836.
[13] E. Todini, Looped water distribution networks design using a resilience index based heuristic approach, Urban Water J. 2 (3) (2000) 115–122.
[14] T. Tanyimboh, M. Tabesh, R. Burrows, Appraisal of source head methods for calculating reliability of water distribution networks, J. Water Res. Plan. Manage. 127 (4) (2001) 206–213.
[15] V.P. Singh, J. Oh, A tsallis entropy-based redundancy measure for water distribution networks, Physica A 421 (2015) 360–376.
[16] R.M. Dziedzic, B.W. Karney, Water distribution system performance metrics, Procedia Eng. 89 (2014) 363–369.
[17] R. Greco, A. Di Nardo, G. Santonastaso, Resilience and entropy as indices of robustness of water distribution networks, J. Hydroinform. 14 (3) (2012) 761–771.
[18] N. Jayaram, K. Srinivasan, Performance-based optimal design and rehabilitation of water distribution networks using life cycle costing, Water Resour. Res. 44 (1) (2008) 1–15.
[19] E. Creaco, M. Franchini, E. Todini, The combined use of resilience and loop diameter uniformity as a good indirect measure of network reliability, Urban Water J. 13 (2) (2014) 167–181.
[20] J.B. Chen, J. Li, Dynamic response and reliability analysis of non-linear stochastic structures, Probab. Eng. Mech. 20 (1) (2005) 33–44.
[21] J. Li, J.B. Chen, The probability density evolution method for dynamic response analysis of non-linear stochastic structures, Internat. J. Numer. Methods Engrg. 65 (6) (2006) 882–903.
[22] U. Shamir, C.D.D. Howard, An analytic approach to scheduling pipe replacement, J. Am. Water Work Assoc. 71 (5) (1979) 248–258.
[23] S. Yamijala, S.D. Guikema, K. Brumbelow, Statistical models for the analysis of water distribution system pipe break data, Reliab. Eng. Syst. Saf. 94 (2) (2009) 282–293.
[24] B.Y. Zhuang, K. Lansey, D. Kang, Resilience/availability analysis of municipal water distribution system incorporating adaptive pump operation, J. Hydraul. Eng.-ASCE 139 (5) (2013) 527–537.
[25] O. Giustolisi, D. Savic, Identification of segments and optimal isolation valve system design in water distribution networks, Urban Water J. 7 (1) (2010) 1–15.
[26] W.W. Sharp, T.M. Walski, Predicting internal roughness in water mains, J. Am. Water Work Assoc. 80 (11) (1988) 34–40.
[27] S.X. Yan, H.B. Zhao, Theory and Calculations of Water Distribution Systems, China Architecture and Building Press, Beijing, 1986, (in Chinese).
[28] Ministry of Housing and Urban-Rural Development of the People's Republic of China, Unified Standard for Reliability Design of Engineering Structures, China Architecture and Building Press, Beijing, 2008, (in Chinese).
[29] J. Li, J.B. Chen, W.L. Sun, Y.B. Peng, Advances of the probability density evolution method for nonlinear stochastic systems, Probab. Eng. Mech. 28 (2012) 132–142.
[30] J.B. Chen, J. Li, The extreme value distribution and dynamic reliability analysis of nonlinear structures with uncertain parameters, Struct. Saf. 29 (2) (2007) 77–93.

[31] J.B. Chen, J. Li, Extreme value distribution and reliability of nonlinear stochastic structures, Earthq. Eng. Eng. Vib. 4 (2) (2005) 275–286.
[32] W. Liu, Z.C. Li, Z.Y. Song, J. Li, Seismic reliability evaluation of gas supply networks based on the probability density evolution method, Struct. Saf. 70 (2018) 21–34.
[33] Ministry of Housing and Urban-Rural Development of People's Republic of Chinaa, Technical Code for Water Supply and Sewerage of Urban, Architecture and Building Press, Beijing, 2012, (in Chinese).
[34] J.B. Chen, J.Y. Yang, J. Li, A GF-discrepancy for point selection in stochastic seismic response analysis of structures with uncertain parameters, Struct. Saf. 59 (2016) 20–31.